International Engineering Journal For Research & Development
Vol.3
Issue 2

e-Skateboard with motion sensing

Sanjay Raj, Rajesh kumar,Rakesh R. Poojari
Assistant Professor
Department of Mechanical Engineering
ARMIET,Thane, India

Abstract - This paper presents the development of a novel air-gliding (hovering) "skateboard" (or "skim-board") which operates based on an aerodynamic principle that distributes airflow uniformly between the board and a flat surface to provide an effective air-bearing for air-gliding. Experiments were parametrically conducted to understand the aerodynamic hovering principle as well as to characterize the performance of the hovering system. We have built several prototypes of the hovering system and showed that it is possible for a board with surface area of ~1mx0.3m (weighing ~5Kg) to glide in air with a rider of ~50Kg on top of it. Besides the obvious fun application of using this hovering board as a skateboard that requires no wheels, another example of applications is to use it as an 'air-skimming' board – when a rider takes a running start and jump onto the board, the board is able to glide with the rider on top of it for several meters. This 'air-skimming' board concept is similar to skim-boarding on a thin-sheet of water that is popular with young adults in many parts of the world. The basic design methodology and performance characteristics of this novel land transport system are described in this paper.

Index Terms – Hoverboard, Air-Gliding, Air-Skimming

I. INTRODUCTION

Ever since the "hovering skateboard" (a levitating skateboard without wheels) appeared in the film *Back to the Future Part II* in 1989, skating enthusiasts have been dreaming about transporting themselves and performing radical maneuvers on a board that floats and glides in air. Inspired by this science-fiction "hovering skateboard", our group is developing an air-gliding transport system to possibly make this dream come true for many kids and adults across the world. We believe that, due to recent advances in several areas of technology, it is now possible to mechatronically integrate a battery-powered hovering system that is capable of carrying the weight of an average adult and allow a rider to be transported in a thin "air-bearing" above the ground. The technologies that will enable the eventual mass-market development of this air-gliding board include powerful electrically driven motors to produce enough aerodynamic lift, new energy-storage systems to allow a reasonable duration of ride (i.e., >20min), and MEMS sensors that are light weight and small enough to be embedded in a hovering system to provide critical feedback information to the motor, which would then be controlled to give more efficient and stable aerodynamic lift to the overall system.

For the lack of a better word, we will refer to the hovering system developed by our group also as a "Hoverboard" – a term that is widely used to describe the hovering skate board that appeared in *Back to the Future Part II*. Hoverboard enthusiasts from all over the world are attempting to realize their dream of gliding on air through different approaches. Two existing successful air-gliding systems are the Airboard developed by Arbortech Company [1] and the homemade DIY hoverboards [2]. The Airboard is the first commercially-marketed hoverboard, which was first introduced in the opening ceremony of the 2000 Olympic Games. However, the Airboard is essentially a sized-down hovercraft, which works using the exact same principle as conventional hovercrafts, and hence it is heavy and consumes much power. It is in the shape of a disk with diameter of 1.6m and height of 0.3m (not including a handle that is attached to the system). The Airboard is run by gasoline and has a 70Kg net system weight.

The existing homemade DIY hoverboards operate based on a new hovering principle which will be introduced in the next section. These DIY hoverboards are usually made by hoverboard enthusiasts and are of low efficiency and stability. The *Hoverboard* discussed in this paper glides in a thin air-bearing (~2mm above the ground) and essentially uses the same hovering principle, but we have drastically improved the efficiency and stability of the existing systems using novel designs to aerodynamically lift the board. Also, to the best of our knowledge, all of the existing hoverboards are powered by either petrol leaf blower or wired blowers, thus making them unfriendly to the environment and impossible to carry around. We will present our demonstration of a prototype electric-powered hoverboard that can carry a person of ~50Kg and glide in air for a few meters with a single arm push-force (the board is about the same size of a commercial snowboard). The Hoverboard can currently be operated in two modes: 1) be ridden like a skateboard, i.e., a rider could put 1 foot on it while the other foot peddles on the ground to propel the board forward just like a skateboard; 2) be ridden like a skim-board, i.e., a person could run and jump on it and the hovering system (with the rider on top of it) would glide on air just like a skim-board that glides on a thin sheet of water.

II. HOVERING PRINCIPLE

The hovering principle used to lift the Hoverboard is basically the same principle presented in [3]. Fig.1 shows the basic steps that the Hoverboard goes through before it "hovers up". The Hoverboard is composed of a base board with an air inlet, a flexible cushion with air outlets, and a *hook-up* board placed at the center of the Hoverboard. When the Hoverboard is placed on a flat ground surface and no air goes into the air inlet, the cushion is not inflated and remains as a flat

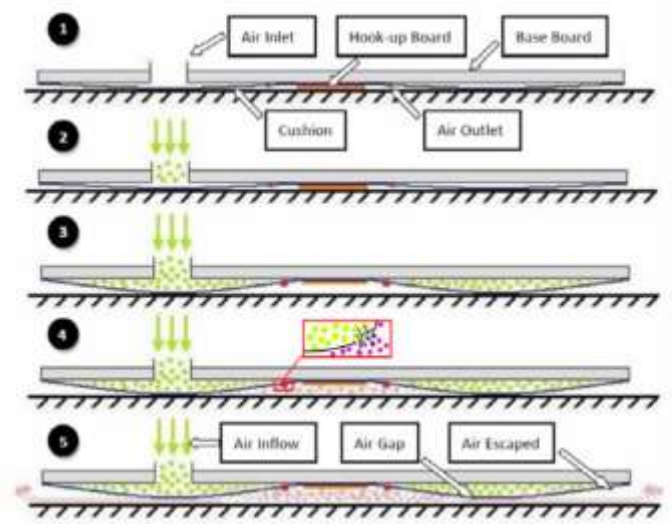

Fig.1 Hovering principle of the Hoverboard.

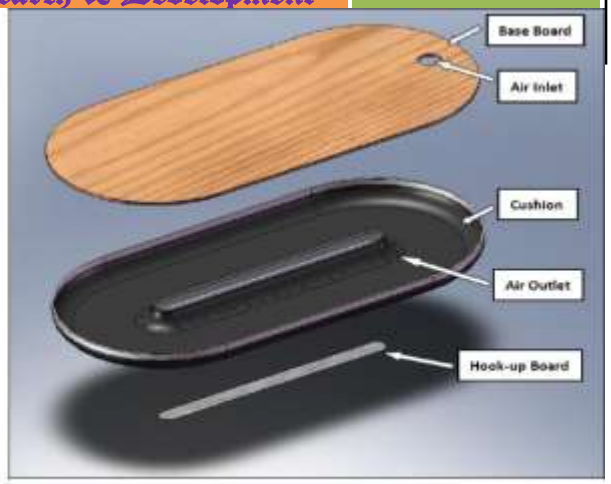

Fig.2 Conceptual illustration of the Hoverboard components

sheet underneath the board. As air is continuously blown into the air inlet by a turbine fan, the air will quickly fill up the enclosed area between the board and the flexible cushion, and eventually inflate the entire cushion into an oval donut shape. With the pressure in the cushion increased to a certain limit (the limit is dependent on the weight of the systems and the number and size of the outlet holes), air will leak out from the outlets placed near the cushion centre. The escaped air will eventually create an air-bearing between the cushion and the ground as shown in Fig. 1-(5). This thin air-bearing will minimize the friction between the Hoverboard and ground.

III. HOVERBOARD STRUCTURE

Different from conventional hovercrafts, the Hoverboard is composed of few simple structures which makes it light in weight and thus easy to carry around, i.e., like a surfboard or snowboard. As stated earlier, the Hoverboard consists of three main components: the board on which a rider stands on, a custom-built flexible cushion that optimizes aerodynamic lift to create an air-bearing, and an electric air blower to provide air flow. To test various geometric configurations of the board, a cordless leaf blower is currently used to provide air flow for evaluating all the Hoverboard models. The blower used in the experiments could provide a maximum flow rate of 120mph with an input voltage of 18V.

The basic mechanical components of the Hoverboard are shown in Fig.2. The base board is the main structure of the Hoverboard on which a rider can stand on. Theoretically, it can be made in any shape with any material that will not leak air. For the ease of fabrication, the base boards of all our prototypes were made with plywood, but with several different shapes. The base board also has a hole to serve as the air inlet of the Hoverboard.

The flexible cushion is the most crucial component of the Hoverboard, i.e., its design determines the aerodynamic lift characteristics of the Hoverboard. It is made with inflatable PVC coated tarpaulin fabric and contains small holes (~2cm diameter) drilled around its centre for the purpose of allowing air to exit the cushion. As well be discussed later in this paper, the number and locations of these outlet holes are extremely important in determining the lift efficiency and stability of the Hoverboard.

The “hook-up board” is made of an aluminium sheet placed underneath the flexible cushion to fix the centre of the cushion on to the base board such that the cushion will be in the shape of a “donut” when inflated. This “donut” shaped area of the cushion is critical in providing pressure force to balance the sum of gravitational forces from the rider and the Hoverboard.

IV. HOVERING THEORY FORMULATION

For the Hoverboard system, the only “hover-force” to offset the gravitational force acting on the board and the person standing on it is the aerodynamic lift-force generated by the air blower flow which is redirected through the outlet holes. Assume the air blower used in our experiments has a
fixed power P_{blower}, the power P used to lift up the board and its rider is the effective power which can be represented by the following equation:

$$P=\eta P_{blower} \qquad (1)$$

where η is the overall efficiency of the hovering system. Now, we propose the following equation to estimate the power required to lift up the Hoverboard and its payload (which is based on existing theories to predict the lift of a conventional hovercraft):

$$P = n\, d\, G\, V_g\, (L_l + L_w)/(L_l\, L_w) \qquad (2)$$

where n is a coefficient, d is the clearance between the board and ground, G is the weight of the board including the payload, L_l is the length of the contour area, L_w is the width of the contour area (i.e., area where the air-bearing separates the board from a flat surface), and V_g is the velocity of the air escaped from the gap between the Hoverboard and ground

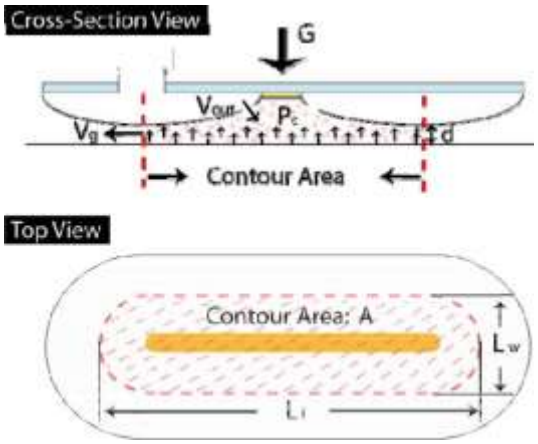

Fig.3 Critical parameters in designing the Hoverboard.

(details are as shown in Fig.3). From (2), the following relationships are observed:

$$P \propto G;\ P \propto V_g\ ;\ P \propto (L_l + L_w)/(L_l\, L_w) \quad (3)$$

Thus, the required power to support the Hoverboard and its payload is directly proportional to the velocity of the air escaped from the gap between the cushion and the ground surface, and also proportional to a function of the cushion geometry. In other words, in order to increase the efficiency of the hovering system, a board with a smaller cushion contour area is desired. In addition, note that it is desirable to have a high exit velocity of the outlet flow from the cushion. cushion dimensions, including the location and number of outlet holes under the cushion. We present only one example here to demonstrate the typical performance of the Hoverboard. We will present the experimental results of all configurations tested at the conference. The physical parameters of this prototype are shown in Table I.

A. Gliding on Air

The no-loading (no rider on top of the board) glide test
targets to prove the floating phenomenon of the Hoverboard and characterize its aerodynamic stability. The experiment was carried out on a smooth ground of a hallway.

After switching on the electric blower at the inlet, the Hoverboard floated up from the ground immediately. With a gentle push at the backend of the board, the Hoverboard started to glide forward and stopped when it contacted a wall 10 meters away from the starting point. The following sequential pictures (Fig. 4) show the movement of the Hoverboard during this gliding process within the first 3 seconds.

B. Gliding on Air with a Rider

This experiment was again carried out on a smooth ground. The rider weighs ~60Kg in this experiment. As shown in Fig.5, a rider pushes the Hoverboard with a running start and then jumps on top of it. The board with the rider then

TABLE I

PHYSICAL PARAMETERS OF THE TESTED HOVERBOARD

Dimension – Length	
Dimension – Width	55 mm
Dimension – Height (Cushion Included)	18 mm
Weight – Board	4 kg
Weight – Blower	6.1 kg

The following equations explain the above statement. Since,

$$P_c = G/A \quad (4)$$

and

$$P_c \propto V_q \propto V_{out}, \quad (5)$$

then, from (4) and (5):

$$G/A \propto V_{out} \quad (6)$$

where P_c is defined as the air pressure between the cushion and ground, V_{out} is the velocity of air coming out from the outlet holes on the cushion, and A is the contour area of the cushion which is proportional to the size of the cushion and equal to $L_l L_w$ in this case.

Thus, the following relationship is true:

$$G/(L_l L_w) \quad V_{out} \quad (7)$$

This implies that if the outlet air velocity is increased, then the size of the board can be decreased to carry the same G without having any negative effects on the hovering performance.

V. Experimental Results

In order to analyze the performance of the Hoverboard, the following experiments were carried out. We have made the Hoverboard with several configurations of its board and glides on the air-bearing for several meters on a flat surface. This is similar to a skim-board rider skimming across a thin sheet of water. In the near future, we envision a Hoverboard rider can glide effortlessly on a flat street surface as shown in Fig.6.

C. Effective Friction Force on the Hoverboard

To quantify the hovering performance of the Hoverboard, the following experiments were conducted to estimate the coefficient of static and kinetic friction of the air-gliding system.

Static Friction Coefficient

As defined, *static friction* is the value of frictional force that a body must overcome in order for it to be set in motion on a flat surface. We used a force gauge (Lutron FG-500) to measure this force in our experiments. During the experiment, the Hoverboard (no-loading) was lifted up aerodynamically first and the force gauge was then placed at the front of the hovering system to apply a force to initiate the movement of

Fig.5 Sequential pictures showing the Hoverboard gliding on air while transporting a person weighing ~60Kg

TABLE II EXPERIMENTAL RESULTS AND COEFFICIENT OF STATIC FRICTION

No. of Experiment	Force Measured (N)	Normal Force N (N)	Coefficient of Static Friction
1st	0.893	99.1	0.0090
2nd	0.863	99.1	0.0087
3rd	0.873	99.1	0.0088
Average			**0.0088**

the system. When the Hoverboard was just on the verge of gliding on the ground, the measurement from the force gauge (F) was recorded. The forces exerted on the Hoverboard in the horizontal direction were simply the push-force exerted by the force gauge and the reacting static friction. Equation (8) shows the classical approximation of the force of friction between two solid surfaces.

$$F=\mu N \qquad (8)$$

where μ is the coefficient of static friction, N is the normal force exerted between the Hoverboard and the ground which in this case was measured to be 99.1N, and F is the friction force between the two surfaces, the magnitude of which equals to the static force measured by the force gauge. Thus the coefficient of static friction can simply be calculated by (9):

$$\mu=F/N \qquad (9)$$

Table II shows the data recorded and the coefficient of static friction calculated, i.e., μ is ~0.0088 for the Hoverboard.

Kinetic Friction Experiment

Kinetic (or dynamic) friction occurs when two objects are moving relative to each other and rub against each other (like a sled sliding on snow). The following method was used to determine the *effective kinetic friction* of the hovering system, i.e., how much does the air-bearing reduce the frictional force between the moving board and the ground. As shown in Fig.7, a propeller was placed at one end of the Hoverboard to provide a constant propelling force. In order to measure the kinetic friction force of the system, the Hoverboard (no-loading) was switched on and followed but powering on the propeller. At the same time, the force gauge was placed at the front of the Hoverboard to apply a force to resist the system from moving forward. When the propeller was rotating at its maximum rotation speed, the measurement from the force gauge was recorded. Hence, this reading gives the approximate propulsion force generated by the propeller throughout the process. The force gauge was then taken away and the hovering system was allowed to move forward by itself. The time required for the hoverboard to move a distance of 7 meters was recorded to calculate the coefficient of the kinetic friction.

Since this is a dynamic case, the frictional force can be calculated through the following approach. In classical mechanics, the distance an object moves has the following relationship with its initial velocity, its acceleration, and the

Fluid simulation was conducted using COSMOS Floworks 2007. The model used in the simulation was built with the exact geometric dimensions as the prototype hoverboard. The only variables in the simulation were the

D. Fluid Flow Analysis

As mentioned earlier, during our development process, many Hoverboard prototypes were built. Even when the sizes of the boards are exactly the same, a slight change in the air outlet holes locations could vary their hovering performance significantly. Motivated by this observation, we conducted fluidic simulations aiming to find the relationship between the number of air outlet holes and their locations in determining the Hoverboard performance.

The coefficient of kinetic friction of the hovering system calculated using (14) is ~0.0034 and the summarized experiment results are shown in Table III.

$$f = F- [(2 L M_{hoverboard}) / t^2]$$
$$\mu= \{F- [(2 L M_{hoverboard}) / t^2]\}/N$$

where: $M_{hoverboard} = 10.1$ ***kg.***

time it travelled:

$$L=V_0t+ (1/2)at^2 = (1/2)at^2 \qquad (10)$$

where L is the distance travelled, V_0 is the initial velocity (in this case is zero), t is the time travelled, and a is the acceleration of the object. Also, since the acceleration a is

related to the force F_{object} exerted on the object and its mass m (assumed to be constant) by way of Newton's second law:

$$F_{object} = ma \quad (11)$$

$$F_{object} = F - f \quad (12)$$

where f is the force of kinetic friction, and F is the force generated by the propeller. Hence, locations and number of air outlets. The ideal design for the outlet holes would be that the air flow inside the cushion is evenly distributed so that the air velocity exiting the outlets are constant and do not vary from hole-to-hole. In addition, a perfect design would allow the outlet flow velocity of each hole to be as high as possible with a given inlet flow.

Variance in Distance to the Center (d)

The first set of simulation was carried out by fixing the number of air outlets to 38 but varying the distance of the holes to the centre. The inlet air velocity was set to be 120mph. The air velocity going out from each of the air outlets were calculated. Since the result is symmetric, thus only half of the results (air outlet number 1 to 20 as indicated in Fig.8) are plotted in Fig. 9 (13) In Fig. 9, the x-axis represents the hole number (as indicated in Fig.8) while the y-axis is the outlet velocity in (14) m/s. As shown in Fig. 9, although the 40mm model has the highest average outlet velocity, the variance of velocity between different holes is very severe which would result in an unbalanced air flow distribution at the bottom of the Hoverboard. Also, clearly, the simulation results indicate that the 50mm and 55mm configurations would provide the worst hovering performance because the outlet velocities are relatively low and fluctuations are relatively large. Based on Fig. 9, the 60mm configuration would provide a relatively good hovering performance in terms of outlet velocity and stability.

The results of the above flow simulation of the hovering system clearly proves that for a Hoverboard size of 115cm x55cm, with 38 air outlets, the optimized distance from the outlet to the centre should be ~60mm. Under this configuration, the average outlet velocity is ~108m/s. Through the above analysis and subsiquent experiments, we have proved that it is possible increase the outlet velocity significantly (using the same input air source) by simply adjusting the outlet locations, i.e., the efficiency of the hovering system could be almost doubled theoretically.

Fig. 10 shows the flow streamline inside the cushion for the 60mm configuration which indicates that the flow is evenly distributed uniformly inside the inflated cushion. We note here that this simulation result coincides with our experimental result in which the 60mm configured prototype stands out to be the most well-performaned one in terms of aerodynamic stability and amount of loading it can lift up.

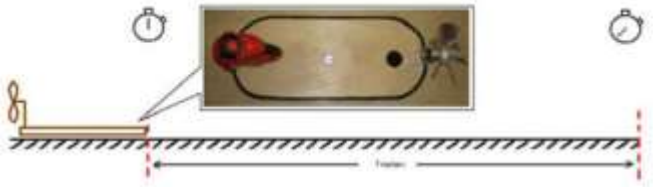

No. of Experience	Propelling Force Measured (N)	Distance Traveled (m)	Normal Force N (N)	Time Spend (s)	Coefficient of Kinetic Friction
1st	7.36	7	99.1	4.48	0.0032
2nd	7.34	7	99.1	4.51	0.0039
3rd	7.43	7	99.1	4.46	0.0032
Average					**0.0034**

Fig.8 Geometric considerations for the fluid dynamic simulation model.

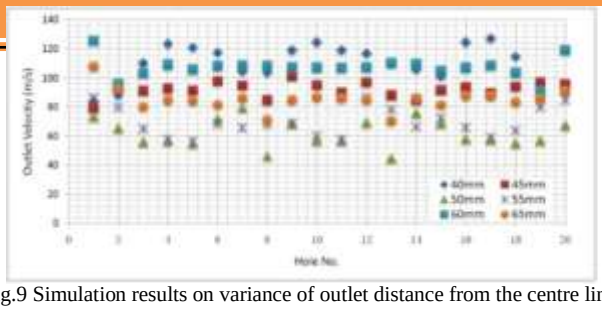

Fig.9 Simulation results on variance of outlet distance from the centre line.

Fig.10 Streamline of the airflow inside the Hoverboard cushion.

Fig.11 Vibration data collection experimental setup.

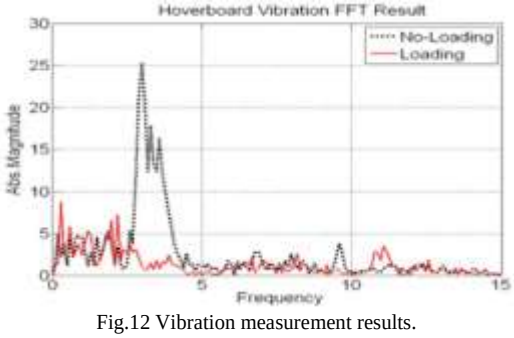

Fig.12 Vibration measurement results.

Variance in Number of Holes

Another parameter that affects the performance of the Hoverboard is the number of air outlets. In this simulation, the number of air outlets were varied from 32 to 52. The reason for conducting this simulation is to find whether increasing in the outlet density will help to lower the air velocity variance between different outlets. The simulation result shown in Table IV indicates that the outlet velocity variance could indeed be reduced by choosing the proper number of holes. Future work is required to investigate whether this effect is coupled with the outlet locations from the centre of the board (i.e., as shown in Fig. 9), and whether an optimal configuration exists for the number and locations of outlet holes for a given Hoverboard size.

Result

We have also integrated motion sensors (to measure vibration/acceleration) on the Hoverboard to measure its vibration during different operation modes. Our future plan is to integrate MEMS sensor and advanced control systems to enhance the capability of the Hoverboard. In this experiment, a wireless sensor mote provided by Virtus Asia Ltd. (Hong Kong), was used to collect vibration data from the Hoverboard. The vibration data were sent in real-time to a PC via Bluetooth protocol, as illustrated in Fig.11. We note here that real-time monitoring of the vibration state of the Hoverboard is important because at certain critical input flow rates, aerodynamic fluttering may be induced on the flexible cushion, and hence cause unwanted vibrations and acoustic

TABLE IV
SIMULATION RESULT WITH VARIANCE IN NUMBER OF OUTLETS

No. of Outlets	Air Outlet Velocity Standard Deviation
32	9.6
34	4.5
38	7.0
44	3.7
52	7.7

noise. Hence, in the future, the measured MEMS sensor signal could be used to control the input air flow rate to avoid fluttering of the cushion.

Fig.12 compares the FFT-processed vibration signals of the Hoverboard with and without loading (i.e., with and without a rider on top of the board). The results show that when the Hoverboard is without loading, the board vibrates at a dominate frequency of 3Hz with a relatively high magnitude. However, when a loading is on top of the Hoverboard, then no such dominate frequency can be observed. The difference in vibration magnitude clearly shows that the board is more stable when a rider is on it. Such difference in MEMS sensor signal will allows us to differentiate the loading status of the Hoverboard and design a more advanced control system for it in the future.

Conclusion

This paper presents a novel *air-gliding board* (*the Hoverboard*) which operates based on a new hovering principle that is different from conventional hovercraft technologies. Experiments were carried out to prove the operability of the Hoverboard. Fluid flow simulations were further performed to determine a possible optimized configuration in distributing air outlets under the

board to maximize its aerodynamic lift and stability. In the future, we plan to integrate MEMS sensors and advanced control systems to further enhance the performance of the Hoverboard.

ACKNOWLEDGMENT

This project is funded by the Centre for Micro and Nano Systems of The Chinese University of Hong Kong and by Virtus Asia Ltd. (Hong Kong).

REFERENCES

[1] Robert L Boylestad and Louis Nashelsky, "Electronic Device And Circuit Theory" ,8th edition 2006.

[2] MrLokesh Mehta, Mr. Pawan Sharma "Spy Night Vision Robot with Moving Wireless Video Camera". International journal of research in engineering technology and management (IJRETM), 2014.

[3] The 8051 microcontroller and embedded system using assembly and C, 2nd edition (ISBN: 9780131194021) by Mazidi Muhammad Ali (2008).

[4] Dhiraj Singh Patel "Mobile Operated Spy Robot" International journal of emerging technology and advanced engineering (IJETAE), 2013.

[5] IEEE xplore http://ieeexplore.ieee.org/search